Scilight

Natural Products Analysis

https://www.sciltp.com/journals/npa

Article

GC–MS–Identified Phytochemicals from *Dimocarpus longan* Leaves as Promising HER2 Inhibitors for Breast Cancer: Molecular Docking, ADMET, and Toxicity Assessment

As-Sazzad Mahmud [1,2,*], Md. Fozla Rabby [1], Md. Foyzur Rahman [1] and Anwara Begum [1]

[1] Department of Pharmacy, Dhaka International University, Satarkul, Badda, Dhaka 1212, Bangladesh
[2] Pharmacy Discipline, Khulna University, Khulna 9208, Bangladesh
* Correspondence: sazzad.phar@diu.ac or sazzadnishan96@gmail.com; Tel.: +88-01521305611

How To Cite: Mahmud, A.-S.; Rabby, D.F.; Rahman, M.F.; et al. GC–MS–Identified Phytochemicals from Dimocarpus longan Leaves as Promising HER2 Inhibitors for Breast Cancer: Molecular Docking, ADMET, and Toxicity Assessment. *Natural Products Analysis* **2026**, *2*(1), 100002. https://doi.org/10.53941/npa.2026.100002

Received: 21 January 2026
Revised: 3 March 2026
Accepted: 3 March 2026
Published: 24 March 2026

Abstract: Breast cancer is still a leading cause of cancer-related deaths globally, and human epidermal growth factor receptor 2 (HER2) overexpression is known to be associated with aggressive tumor characteristics and drug resistance. Although the development of clinically used HER2 inhibitors has shown improved outcomes for patients, their efficacy is often hampered by factors such as low bioavailability, drug resistance, and toxicity. In this research, the leaves of *Dimocarpus longan* were investigated as a natural source of new lead compounds for the development of next-generation HER2 inhibitors. Phytochemicals isolated from methanolic extracts of the leaves were assessed using an integrated computational approach that included molecular docking, pharmacokinetic analysis, toxicity prediction, and structure-activity relationship analysis. Some phytocompounds showed positive binding affinity interactions with the HER2 kinase domain, displaying affinity interaction profiles similar to known HER2 kinase inhibitors, including essential hydrogen bonding and hydrophobic interactions in the active site. *In silico* pharmacokinetic analysis showed that many compounds had desirable drug-likeness properties, including good gastrointestinal absorption and conformance to essential medicinal chemistry guidelines. Moreover, toxicity profiling indicated lower probabilities of hepatic, neurological, and immunological toxicities for some candidates. Structure-activity relationship analysis emphasized the significance of harmonious polar functional groups and hydrophobic cores in potentiating HER2 kinase inhibition. In conclusion, the results suggest that *D. longan*-derived phytocompounds are promising candidates for the development of safer and more bioavailable HER2-targeting drugs. Further experimental verification and rational optimization are required to translate these candidates into potential therapeutic agents for HER2-positive breast cancer.

Keywords: *Dimocarpus longan*; HER2; GC–MS; molecular docking; ADMET; breast cancer

1. Introduction

Breast cancer is a major global health concern and continues to rank among the leading causes of cancer morbidity and mortality. According to the most recent global cancer statistics, more than 2.3 million new cases and approximately 666,000 deaths were recorded in 2022, accounting for nearly one in eight cancer diagnoses

worldwide. Projections suggest that the burden will continue to rise, with an estimated 3.2 million new diagnoses and 1.1 million deaths annually by 2050 [1,2]. Although advances in screening and therapy have improved survival rates, breast cancer remains a pressing clinical and social challenge, particularly in low- and middle-income countries where access to effective therapies is often limited.

Therapeutic approaches for breast cancer have evolved substantially over the last two decades. Standard treatment regimens typically include surgery, chemotherapy, radiotherapy, and targeted therapies. Despite the success of HER2-directed agents such as trastuzumab and lapatinib, issues of drug resistance, toxicity, and limited accessibility remain significant barriers [3]. These limitations highlight the urgent need to explore alternative or complementary therapeutic strategies that are both effective and safer for long-term use.

Among the molecular drivers of breast cancer, the human epidermal growth factor receptor 2 (HER2) plays a central role [4]. HER2 is overexpressed in approximately 20–30% of breast cancer cases, and its amplification is strongly associated with aggressive tumor progression, higher recurrence rates, and poor clinical outcomes [5,6]. Targeting HER2 has therefore become a cornerstone of therapy. However, the drawbacks of existing drugs provide a rationale for the discovery of new HER2 inhibitors, ideally derived from natural, less toxic sources.

Medicinal plants have historically served as a valuable reservoir for anticancer agents, with compounds such as paclitaxel and vincristine originating from natural sources [7]. In this context, *Dimocarpus longan Lour.*, a tropical fruit tree of the Sapindaceae family, has garnered attention for its potential pharmacological properties. Traditionally used in Asian medicine, different parts of the plant, including leaves, pericarp, and seeds, contain bioactive compounds such as flavonoids, phenolic acids, and triterpenoids. Previous studies have demonstrated the antioxidant, anti-inflammatory, immunomodulatory, and cytotoxic activities of *D. longan* extracts against various cancer cell lines [8]. Despite these promising findings, little is known about the direct interaction of *D. longan* phytochemicals with HER2, leaving an important gap in current knowledge.

The present study addresses this gap by identifying phytocompounds from the methanolic extract of *D. longan* leaves using gas chromatography–mass spectrometry (GC–MS), followed by molecular docking and ADMET analyses to assess their potential as HER2 inhibitors. Comparative docking with the synthetic drug lapatinib was performed to evaluate relative binding affinities. By combining *in silico* and preliminary biological insights, this research lays the groundwork for developing *D. longan* derived phytocompounds as novel, plant-based therapeutics for HER2-positive breast cancer.

2. Materials and Methods

2.1. Collection and Extraction of Leaves

Leaves of the *Dimocarpus longan* plant were collected from the Bangladesh National Herbarium in Dhaka in 2024, with identification confirmed by a scientific officer. A specimen is preserved at the Department of Pharmacy, Dhaka International University. After collection, stems and impurities were removed. The fresh leaves were rinsed and air-dried at room temperature (25 ± 2 °C) until completely dry, then ground into a coarse powder using a sanitized blender to prevent contamination. Maceration was carried out by soaking 450 g of the powdered leaves in 3 L of methanol for 10 days with occasional stirring. The mixture was then filtered using Whatman filter paper, and the resulting extract (MEDL) was dried at room temperature. The fresh MEDL was subsequently used for GC-MS analysis.

2.2. GC-MS Analysis

The chromatographic procedure was performed using a GC-MS model MSQP2010 (Shimadzu, Kyoto, Japan) with auto autosampler. 1000 ppm solutions in methanol, ethylacetate, and hexane were prepared from three extracts (methanol, ethylacetate, and hexane), and 1 µL of each extract was injected for analysis using -DB-5MS column (30 m × 0.25 mm, film thickness 0.25 µm). Helium gas was used at a flow rate of 1 mL/min as a carrier gas. The analysis was carried out using oven programming of initial temperature 50 °C for 2 min, followed by a ramp rate of 20 °C/minute up to 130 °C, followed by a ramp of 12 °C/min. to a temperature of 180 °C, finally raised temperature to 280 °C at 3 °C per minute and hold for 15 min. The ion source temperature was set at 250 °C. The injection port temperature was set to 250 °C, and the total run time was 40 min. The instrument was operated in electron impact (EI) mode with an electron energy of 70 eV. Confirmation of analytes was done by SIM (selective ion mode) [9].

2.3. In Silico Studies

2.3.1. Ligand Collection

From the GC–MS analysis of the methanol extract of *Dimocarpus longan*, 64 compounds were identified tentatively. Ligand selection and preparation from the PubChem Database, the standard drug, and 64 compounds (SDF file) from *Dimocarpus longan* were retrieved. The optimization was done with Open Babel and PyRx to prepare them for docking. The PyRx tool was used to convert the ligand (SDF format) to a PDBQT file to generate the atomic coordinates. At a set mmff94 force field, the optimization algorithm was used to minimize the energy to a minimum [8].

2.3.2. Protein Selection and Preparation

The receptors were selected following the parameter criteria in the Ramachandran Plot, Resolution, and R-Value. "The crystal structure of breast cancer protein HER2, PDB ID: 7PCD, resolution of 1.77 Å, and a free R-Value of 0.241, was downloaded from the protein data bank. Next, missing hydrogen atoms were added and the protein using Discovery Studio 2020. In here, all crystallographic water molecules, heteroatoms, and ligands were removed [10]. Finally, Energy minimization is required to stabilize the protein structure, which was ensured utilizing the GROMOS96 force-field of SWISS PDB Viewer accessed on December, 2025 (https://spdbv.unil.ch/) [10].

2.3.3. Molecular Docking

Based on scoring functions, PyRx was used to carry out the molecular docking. PyRx is an open-access virtual screening tool dedicated to the screening of a vast range of libraries of compounds against a particular drug target. AutoDock4 and AutoDock Vina are the two most effective tools under the banner of PyRx, which offer a user-friendly interface to carry out molecular docking for CADD (computer-aided drug design) [8]. This software is characterized by a grid box spacing dimension of 25,25,25 and x, y, and z axes. Ten amino acid mutations identified in the HER2 protein that cause breast cancer, including L755S, S760A, D769H, PV777L, P780ins, L785F, S783P, L785F, S798P, Y835, R838Q, V842I [11]. The grid map with dimensions of 0.2066, 1.3537, and 19.0665 Å was generated that covered the binding pocket of the HER2 protein. The binding affinity score between the phytocompound and the target protein HER2. Here, Lapatinib is a standard drug, which is an oral dual tyrosine kinase inhibitor selective for the inhibition of epidermal growth factor receptor HER2. Having more targets, probably its antitumor activity could be more efficient. Clinical data have shown that lapatinib is active in HER2-positive breast cancer as monotherapy [12].

2.3.4. ADMET Analysis

Prediction of the ADMET profile for drug candidates and environmental chemicals plays a major role in drug discovery. The computational biology tool ADME descriptors assist in the estimation of pharmacokinetic parameters and the assessment of molecular quality based on drug absorption, distribution, metabolism, and excretion. When administered simultaneously, the intensity and time course of PK (ADME) qualities determine the flow of drugs into, through and out of the body. This technique reduces the cost of new medication development as well as the risk of clinical failure. In the early stages of medication research, pharmacokinetic factors help to identify the integrity and efficacy of plant components.

3. Results

3.1. GC-MS Analysis

The methanol extract of *Dimocarpus longan* leaves were analyzed for the chemical constituents using gas chromatography and Mass spectrometry (GC–MS). The characterization of the methanol extract through GC–MS revealed the presence of sixty-four (64) compounds present in it tentatively. The phytochemicals identified with their respective molecular masses, relative percentage, and retention time have been tabulated in Table 1 and Figure 1.

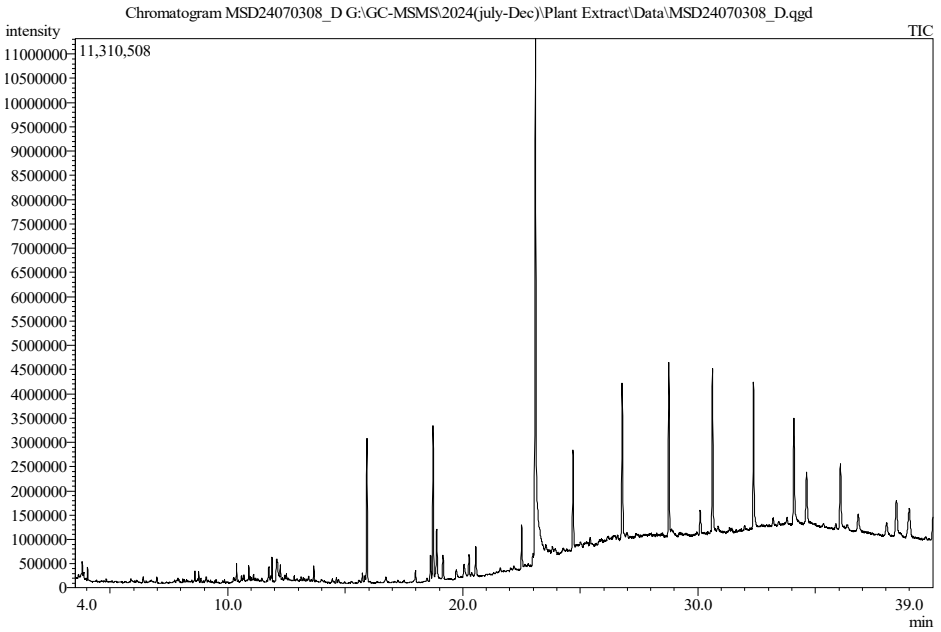

Figure 1. Total Ionic Chromatogram.

Table 1. Biological activity of Phyto-Components identified in Methanolic extract of *Dimocurpus Longan* leaves (GC-MS study).

Serial No	Retention Time	Area %	Compound Name
1	2.699	19.688	3,5-Dithiahexanol 5,5-dioxide
2	2.776	1.491	Trimethylsilyl fluoride
3	3.127	4.347	Propionic acid, 2,3-dihydroxy-3-phenyl-
4	3.863	0.370	2-Propanol, 1,1′-oxybis-
5	3.906	0.220	Succinic acid, 2-(3-nitrophenyl)ethyl tridecyl ester
6	8.603	0.231	Dodecane, 2,6,11-trimethyl-
7	10.892	0.486	Phenol, 3,5-bis(1,1-dimethylethyl)-
8	11.75	0.173	1H-Cycloprop[e]azulen-7-ol, decahydro-1,1,7-trimethyl-4-methylene-, [1ar-(1a.alpha.,4a.alpha.,7.beta.,7a.beta.,7b.alpha.)]-
9	15.922	3.561	Hexadecanoic acid, methyl ester
10	16.062	0.185	Benzenepropanoic acid, 3,5-bis(1,1-dimethylethyl)-4-hydroxy-, methyl ester
11	18.479	0.185	5-Eicosene, (E)-
12	18.632	0.728	Methyl 10,11-octadecadienoate
13	18.734	4.890	8,11,14-Docosatrienoic acid, methyl ester
14	18.89	1.445	Phytol
15	19.158	0.647	Methyl stearate
16	20.057	0.890	Hexadecanamide
17	20.377	0.266	Dihydroartemisinin, 10-O-(t-butyloxy)-
18	20.557	1.006	Methyl 11-docosenoate
19	22.186	0.254	Tetratetracontane
20	22.525	0.243	[1,1′-Bicyclopropyl]-2-octanoic acid, 2′-hexyl-, methyl ester
21	23.087	37.179	9-Octadecenamide, (Z)-
22	23.536	0.439	Carbonic acid, eicosyl prop-1-en-2-yl ester
23	23.661	0.382	11-Methyltricosane
24	23.823	0.566	Octacosane
25	23.935	0.208	1-Bromodocosane
26	24.805	0.647	3,7-Decadien-2-one, 10-(3,3-dimethyloxiranyl)-4,8-dimethyl-, (E,E)-.+/-.-
27	24.934	0.220	2,3:5,6-Di-O-1-Cyclohexylieden-1,4-cyclohexandiallylether
28	25.009	0.994	Eicosyl isopropyl ether
	25.201	0.220	4,11-Dimethyl-8-(propan-2-yl)-5,12-dioxatricyclo[9.1.0.04,6]dodecan-7-ol, Ac
29	25.535	0.185	erythro-7,8-Dichlorodisparlure
30	25.765	0.786	4-Methyldocosane
31	25.904	0.277	Ethanol, 2-(hexadecyloxy)-
32	25.947	0.197	Decane, 5,6-bis(2,2-dimethylpropylidene)-, (E,Z)-

Table 1. *Cont.*

Serial No	Retention Time	Area %	Compound Name
33	26.015	0.474	Dodecanoic acid, 2-penten-1-yl ester
34	26.073	0.208	Hexadecanoic acid, (3-bromoprop-2-ynyl) ester
35	26.145	0.763	Oxiraneoctanoic acid, 3-octyl-, cis-
36	26.275	0.520	Geranyl isovalerate
37	26.37	0.405	9-Undecene-4,6-dione, 3,5,7,10-tetramethyl-
38	26.46	0.728	Z-5-Methyl-6-heneicosen-11-one
39	26.59	0.763	Tetrapentacontane, 1,54-dibromo-
40	26.729	0.301	1-Bromo-11-iodoundecane
41	26.802	0.555	d-Mannitol, 1-O-(22-hydroxydocosyl)-
42	26.865	0.266	1-Heptadec-1-ynyl-cyclopentanol
43	26.91	0.173	4-Cyclohexylpiperidine
44	27.365	0.335	6,10,13-Trimethyltetradecyl isovalerate
45	27.585	0.185	Pentafluoropropionic acid, heptadecyl ester
46	27.693	0.243	E-2-Methyl-3-tetradecen-1-ol acetate
47	28.096	0.197	2-Acetoxy-1,1,10-trimethyl-6,9-epidioxydecalin
48	28.249	0.254	Docosane, 1,22-dibromo-
49	28.335	0.277	erythro-7,8-Bromochlorodisparlure
50	28.892	0.370	Nonahexacontanoic acid
51	28.925	0.220	Dodecyl octyl ether
52	28.985	0.266	Z-8-Methyl-9-tetradecen-1-ol acetate
53	29.199	0.451	tert-Butyl (2-aminophenyl)carbamate, 2TMS derivative
54	29.345	0.243	2H-3,9a-Methano-1-benzoxepin, octahydro-2,2,5a,9-tetramethyl-, [3R-(3.alpha.,5a.alpha.,9.alpha.,9a.alpha.)]-
55	29.595	0.266	Pseudodiosgenin
56	29.918	0.185	Fumaric acid, 2-chloroethyl dodecyl ester
57	29.953	0.266	Disparlure
58	30.11	0.855	Squalene
	33.459	0.289	3-tert-Butylphenol, tert.-butyldimethylsilyl ether
59	33.54	0.405	Naphthalene, decahydro-1,8a-dimethyl-7-(1-methylethyl)-, [1R-(1.alpha.,4a.beta.,7.beta.,8a.alpha.)]-
60	36.83	0.844	22,23-Dibromostigmasterol acetate
61	38.043	0.890	Pregna-5,8-diene-3.beta.,11.alpha.-diol-20-one diacetate
62	39.005	1.457	24-Norursa-3,12-diene
63	34.626	2.405	Vitamin E
64	35.881	0.335	1,1,1,3,3,5,5,7,7,9,9,11,11,13,13,15,15,17,17,19,19,19-docosamethyldecasiloxane

3.2. Molecular Docking

In Table 2, Lapatinib is a standard drug. The binding affinity of lapatinib is −10.5. The top nine ligands have been selected based on best binding capacity for comparison with the standard. Their higher binding affinity suggests that they could effectively inhibit the expression of the HER2 protein [13].

Table 2. Binding Affinity of sample Lapatinib and 9 ligands.

Sl. No	Name	CID ID	Binding Affinity
1	Lapatinib	208908	−10.5
2	Dihydroartemisinin, 10-O-(t-butyloxy)-	537898	−9.3
3	Pseudodiosgenin	10573853	−9.3
4	22,23-Dibromostigmasterol acetate	91691660	−8.9
5	24-Norursa-3,12-diene	91735342	−8.6
6	Pregna-5,8-diene-3.beta.,11.alpha.-diol-20-one diacetate	536856	−8.3
7	2-Acetoxy-1,1,10-trimethyl-6,9-epidioxydecalin	538309	−7.9
8	Naphthalene, decahydro-1,8a-dimethyl-7-(1-methylethyl)-, [1R-(1.alpha.,4a.beta.,7.beta.,8a.alpha.)]-	23619266	−7.5
9	1H-Cycloprop[e]azulen-7-ol, decahydro-1,1,7-trimethyl-4-methylene-, [1ar-(1a.alpha.,4a.alpha.,7.beta.,7a.beta.,7b.alpha.)]-	6432640	−7.5
10	Succinic acid, 2-(3-nitrophenyl)ethyl tridecyl ester	91720247	−7.3

3.3. ADME Analysis

The ADME screening of phytochemicals from *Dimocarpus longan* leaves in comparison with the standard drug Lapatinib demonstrated notable differences in pharmacokinetic behavior. Lapatinib, while effective as a HER2 inhibitor, showed limitations by violating one of Lipinski's rules due to its high molecular weight, which resulted in low gastrointestinal absorption and poor blood–brain barrier permeability. In contrast, several phytocompounds exhibited more favorable pharmacokinetic properties. DHA-tBu (CID 537898) and Pseudodiosgenin (CID 10573853) displayed high gastrointestinal absorption, favorable lipophilicity, and no or minimal Lipinski violations, indicating superior pharmacokinetics compared with Lapatinib. Pregna-5,8-diene-3β,11α-diol-20-one diacetate (CID 536856) fully complied with Lipinski's rules, demonstrating excellent drug-likeness with a predicted intestinal absorption rate of 99.3% and no violations.

On the other hand, 22,23-Dibromostigmasterol acetate (CID 91691660), despite strong docking performance, exhibited two violations related to high molecular weight and lipophilicity, predicting poor absorption and limited permeability. Similarly, 24-Norursa-3,12-diene (CID 91735342) and Deca-Naph-IMe (CID 23619266) showed high lipophilicity but were associated with low gastrointestinal absorption and poor blood–brain barrier permeability, reducing their potential clinical applicability. ATM-EpiDec (CID 538309) and CPA-TMe (CID 6432640) satisfied all of Lipinski's parameters, with high gastrointestinal absorption and no violations, reflecting their strong potential as orally bioavailable candidates. The succinic acid derivative SNTE (CID 91720247) demonstrated moderate compliance; however, the presence of a nitrophenyl group raised mutagenicity concerns despite otherwise acceptable ADME values as mentioned in Table 3.

Overall, DHA-tBu, Pseudodiosgenin, Pregna-5,8-diene-3β,11α-diol-20-one diacetate, ATM-EpiDec, and CPA-TMe emerged as the most promising phytoligands, combining strong docking affinities with favorable ADME profiles. These findings highlight their potential as safer and more bioavailable alternatives to Lapatinib, which suffers from pharmacokinetic limitations that restrict its therapeutic efficiency.

3.4. Toxicity Prediction

The toxicity prediction analysis highlighted distinct differences between the standard drug Lapatinib and the selected phytocompounds. Lapatinib demonstrated multiple toxic liabilities, including hepatotoxicity, neurotoxicity, respiratory toxicity, immunotoxicity, and cytotoxicity, with high probabilities ranging from 0.76 to 0.96. These results align with its known clinical limitations, particularly its hepatotoxic and immunotoxic side effects, which often restrict long-term therapeutic application.

Among the phytoligands, 22,23-Dibromostigmasterol acetate showed lower hepatotoxic and neurotoxic risks compared to Lapatinib but carried a strong probability of immunotoxicity (0.99) and moderate carcinogenicity, suggesting caution in its potential application. Similarly, 24-Norursa-3,12-diene exhibited a more favorable safety profile, with only mild neurotoxic and immunotoxic predictions, while maintaining a lower risk of other organ-related toxicities.

The compound Deca-Naph-IMe (CID 23619266) emerged as one of the least toxic candidates, showing inactive predictions across hepatotoxicity, neurotoxicity, nephrotoxicity, and immunotoxicity, alongside a low probability of carcinogenic and cytotoxic effects. This indicates a relatively safe toxicity profile compared with both Lapatinib and other phytocompounds. In contrast, Succinic acid derivative (CID 91720247) raised significant concerns due to its predicted mutagenicity (0.92) and mild nephrotoxic activity, despite being largely inactive for other toxic endpoints as seen in Table 4.

Overall, while Lapatinib demonstrated multiple active toxicities that could compromise patient safety, several phytocompounds such as 24-Norursa-3,12-diene and Deca-Naph-IMe showed comparatively safer profiles with fewer toxicity liabilities. However, the succinic acid derivative requires careful evaluation due to its mutagenic potential, and 22,23-Dibromostigmasterol acetate presents immunotoxic risks that may limit clinical translation. These findings underscore the importance of integrating toxicity predictions into early-stage drug discovery to balance efficacy with safety.

Table 3. Absorption, distribution, metabolism, and excretion (ADME) of phytoligands and standard drugs.

Name	CID ID	Formula	M.W (g/mol)	H-Bond Acceptors	H-Bond Donors	Lipophilicity	GI Absorption	BBB Permeant	Lipinski	BBB	Water Solubility	Intestinal Absorption
Lapatinib	208908	$C_{29}H_{26}ClFN_4O_4S$	581.06	8	2	4.2	Low	No	Yes; 1 violation	−0.785	−4.324	100
DHA-tBu	537898	$C_{19}H_{32}O_6$	356.45	6	0	3.98	High	Yes	Yes; 0 violation	0.387	−4.732	94.796
PDG	10573853	$C_{27}H_{42}O_3$	414.62	3	2	4.29	High	Yes	Yes; 1 violation	−0.28	−5.168	94.423
DB-StigAc	91691660	$C_{31}H_{50}Br_2O_2$	614.54	2	0	5.65	low	No	No; 2 violations	0.723	−7.142	94.607
NorUrsa-Diene	91735342	$C_{29}H_{46}$	394.68	0	0	4.76	Low	No	Yes; 1 violation	0.269	−4.857	91.722
Preg-Diol-DiAc	536856	$C_{25}H_{34}O_5$	414.53	5	0	3.38	High	yes	Yes; 0 violation	−0.303	−5.09	99.267
ATM-EpiDec	538309	$C_{15}H_{24}O_4$	268.35	4	0	2.75	high	yes	Yes; 0 violation	−0.015	−3.379	96.804
Deca-Naph-IMe	23619266	$C_{15}H_{28}$	208.38	0	0	3.38	Low	No	Yes; 1 violation	0.828	−6.532	95.416
CPA-TMe	6432640	$C_{15}H_{24}O$	220.35	1	1	2.88	High	yes	Yes; 0 violation	0.617	−3.94	93.906
SNTE	91720247	$C_{25}H_{39}NO_6$	449.58	6	0	4.84	Low	No	Yes; 0 violation	−1.1	−6.688	91.465

DHA-tBu = Dihydroartemisinin, 10-O-(t-butyloxy)-; PDG = Pseudodiosgenin; DB-StigAc = 22,23-Dibromostigmasterol acetate; Preg-Diol-DiAc = Pregna-5,8-diene-3β,11α-diol-20-one diacetate; ATM-EpiDec = 2-Acetoxy-1,1,10-trimethyl-6,9-epidioxydecalin; Deca-Naph-IMe = Naphthalene, decahydro-1,8a-dimethyl-7-(1-methylethyl)-; CPA-TMe = 1H-Cycloprop[e]azulen-7-ol, decahydro-1,1,7-trimethyl-4-methylene-; SNTE = Succinic acid, 2-(3-nitrophenyl)ethyl tridecyl ester; NorUrsa-Diene = 24-Norursa-3,12-diene; DDE-DMO = 3,7-Decadien-2-one, 10-(3,3-dimethyloxiranyl)-4,8-dimethyl-, (E,E)-.

Table 4. Toxicity Prediction.

Name	CID ID	Classification	Target	Prediction	Probability
Lapatinib	208908	Organ toxicity	Hepatotoxicity	Active	0.8
		Organ toxicity	Neurotoxicity	Active	0.86
		Organ toxicity	Nephrotoxicity	Inactive	0.8
		Organ toxicity	Respiratory toxicity	Active	0.94
		Organ toxicity	Cardiotoxicity	Inactive	0.75
		Toxicity end points	Carcinogenicity	Inactive	0.55
		Toxicity end points	Immunotoxicity	Active	0.96
		Toxicity end points	Mutagenicity	Inactive	0.51
		Toxicity end points	Cytotoxicity	Active	0.76
DB-StigAc	91691660	Organ toxicity	Hepatotoxicity	Inactive	0.68
		Organ toxicity	Neurotoxicity	Inactive	0.5
		Organ toxicity	Nephrotoxicity	Inactive	0.71
		Organ toxicity	Respiratory toxicity	Active	0.75
		Organ toxicity	Cardiotoxicity	Inactive	0.53
		Toxicity end points	Carcinogenicity	Active	0.55
		Toxicity end points	Immunotoxicity	Active	0.99
		Toxicity end points	Mutagenicity	Inactive	0.93
		Toxicity end points	Cytotoxicity	Inactive	0.66
NorUrsa-Diene	91735342	Organ toxicity	Hepatotoxicity	Inactive	0.78
		Organ toxicity	Neurotoxicity	Active	0.56
		Organ toxicity	Nephrotoxicity	Inactive	0.95
		Organ toxicity	Respiratory toxicity	Inactive	0.72
		Organ toxicity	Cardiotoxicity	Inactive	0.85
		Toxicity end points	Carcinogenicity	Inactive	0.67
		Toxicity end points	Immunotoxicity	Active	0.72
		Toxicity end points	Mutagenicity	Inactive	0.83
		Toxicity end points	Cytotoxicity	Inactive	0.74
Deca-Naph-IMe	23619266	Organ toxicity	Hepatotoxicity	Inactive	0.88
		Organ toxicity	Neurotoxicity	Inactive	0.51
		Organ toxicity	Nephrotoxicity	Inactive	0.93
		Organ toxicity	Respiratory toxicity	Inactive	0.68
		Organ toxicity	Cardiotoxicity	Inactive	0.87
		Toxicity end points	Carcinogenicity	Inactive	0.75
		Toxicity end points	Immunotoxicity	Inactive	0.87
		Toxicity end points	Mutagenicity	Inactive	0.71
		Toxicity end points	Cytotoxicity	Inactive	0.75
SNTE	91720247	Organ toxicity	Hepatotoxicity	Inactive	0.79
		Organ toxicity	Neurotoxicity	Inactive	0.85
		Organ toxicity	Nephrotoxicity	Active	0.51
		Organ toxicity	Respiratory toxicity	Inactive	0.59
		Organ toxicity	Cardiotoxicity	Inactive	0.61
		Toxicity end points	Carcinogenicity	Inactive	0.6
		Toxicity end points	Immunotoxicity	Active	0.57
		Toxicity end points	Mutagenicity	Active	0.92
		Toxicity end points	Cytotoxicity	Inactive	0.78

3.5. Post-Docking Analysis

The interaction analysis between HER2 protein and the ligands revealed diverse bonding patterns, highlighting the mechanistic differences between the standard drug Lapatinib and the selected phytocompounds.

Lapatinib exhibited a combination of hydrogen bonding, electrostatic, and hydrophobic interactions, including conventional hydrogen bonds with MET801, ASP863, and ASP845, as well as electrostatic interactions with LYS753. Additionally, multiple hydrophobic interactions involving residues such as LEU726, VAL734, PHE864, and ILE767 were observed, which collectively stabilize its binding within the HER2 active site. This broad interaction spectrum explains the strong binding affinity of Lapatinib.

In contrast, 22,23-Dibromostigmasterol acetate primarily formed hydrophobic interactions, especially with LEU852, LEU726, VAL734, ALA771, ALA751, and PHE864, with several Pi-alkyl contacts contributing to stabilization. Although it lacked conventional hydrogen bonds, the abundance of alkyl and Pi-alkyl interactions suggests stable hydrophobic embedding within the HER2 binding cavity.

The compound 24-Norursa-3,12-diene also relied exclusively on hydrophobic alkyl interactions, engaging residues such as LEU712, ARG713, ARG784, and LEU786. The repetitive involvement of ARG713 and ARG784 indicates selective hydrophobic anchoring at the receptor interface.

Naphthalene, decahydro-1,8a-dimethyl-7-(1-methylethyl)- displayed a similar hydrophobic interaction profile, involving ALA771, LEU785, LEU796, and PHE864, with Pi-alkyl interactions further enhancing binding stability.

Succinic acid, 2-(3-nitrophenyl) ethyl tridecyl ester, in contrast, demonstrated a more diverse interaction profile compared to other phytocompounds. It formed multiple hydrogen bonds with residues LYS753, SER783, and THR862, along with additional carbon hydrogen bonds. Moreover, strong hydrophobic interactions with residues such as VAL734, ALA751, LEU852, LEU726, LEU800, MET801, and PHE864 contributed to its stabilization. The combination of both polar and nonpolar interactions in this ligand suggests a binding pattern closer to that of Lapatinib.

Overall, while Lapatinib displayed a balance of hydrogen bonding, electrostatic, and hydrophobic interactions, most phytocompounds primarily relied on hydrophobic stabilization, except the succinic acid derivative, which exhibited both hydrogen bonding and hydrophobic contacts Figure 2 and Table 5. This indicates that phytoligands can effectively interact with HER2, but with distinct mechanisms compared to the standard drug, potentially offering alternative modes of receptor modulation.

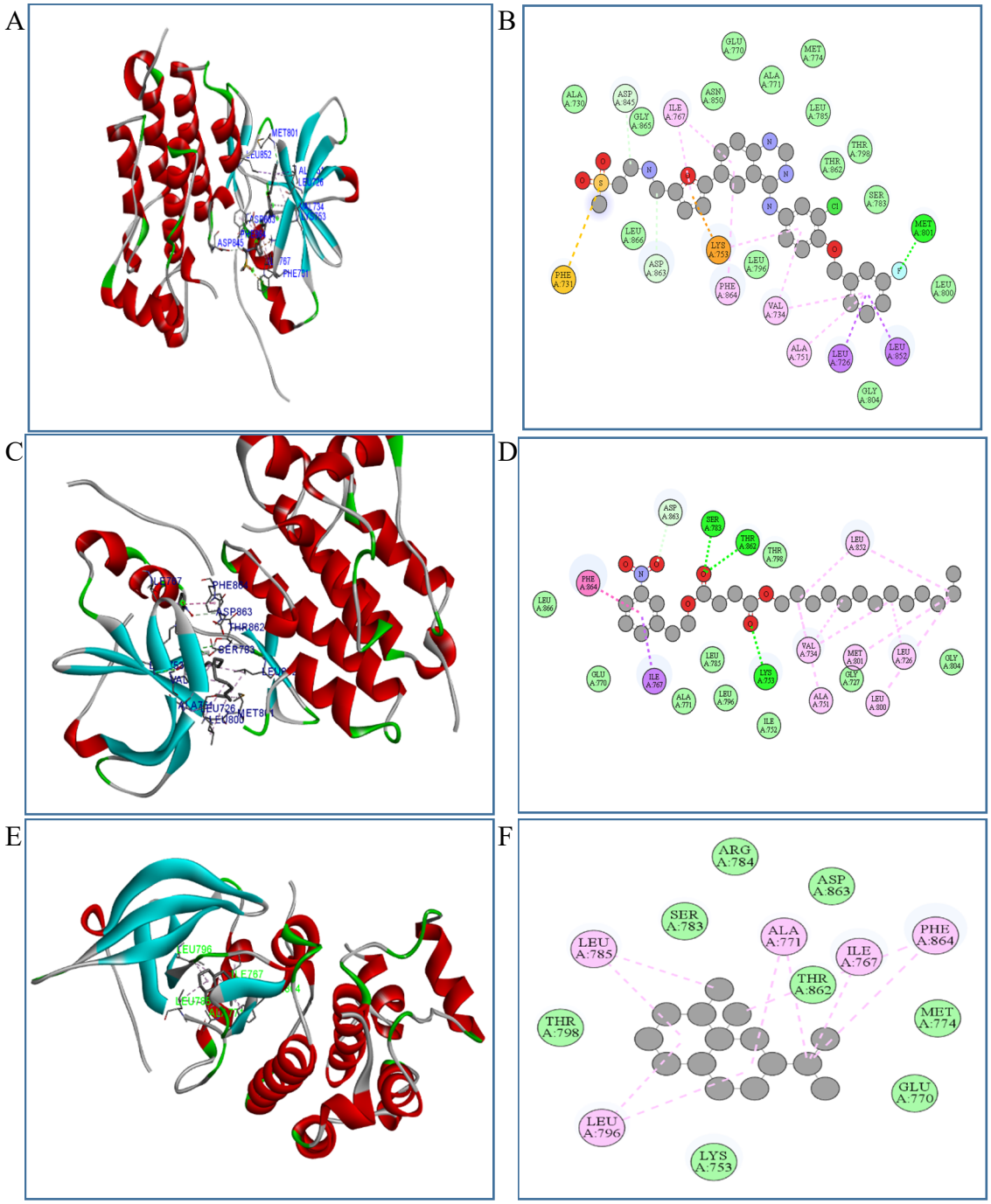

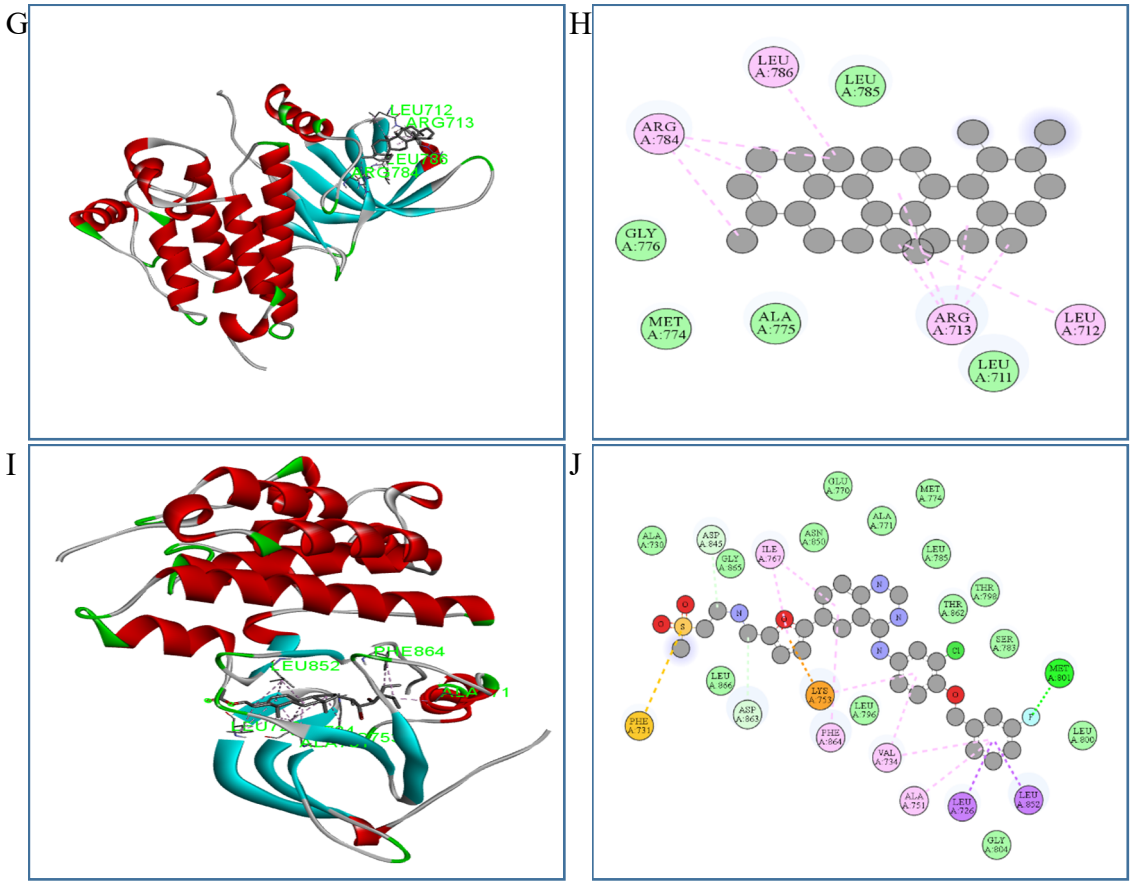

Figure 2. (**A**,**B**) is 2D &3D picture in interaction between HER2 protein and standard drug Lapatinib; (**C**,**D**) is 2D &3D picture in interaction between HER2 protein and ligand Succinic acid, 2-(3-nitrophenyl)ethyl tridecyl ester; (**E**,**F**) is picture in interaction between HER2 protein and ligand Naphthalene, decahydro-1,8a-dimethyl-7-(1-methylethyl)-, [1R-(1.alpha.,4a.beta.,7.beta.,8a.alpha.)]; (**G**,**H**) is picture in interaction between HER2 protein and ligand 24-Norursa-3,12-diene; (**I**,**J**) is picture in interaction between HER2 protein and ligand 22,23-Dibromostigmasterol acetate.

Table 5. List of bond interactions between target proteins (HER2) and ligands (plant compounds).

Ligand	Residues	Distance (Å)	Category Bond	Type
Lapatinib	MET801	2.03596	Hydrogen Bond	Conventional Hydrogen
	ASP863	3.29581	Hydrogen Bond	Conventional Hydrogen
	ASP845	3.23502	Hydrogen Bond	Carbon Hydrogen
	LYS753	3.49778	Electrostatic	Carbon Hydrogen
	LEU726	3.95598	Hydrophobic	Pi-Cation
	LEU852	3.8388	Hydrophobic	Pi-Sigma
	PHE731	5.70695	Other	Pi-Sigma
	ILE767	5.17187	Hydrophobic	Pi-Sulfur
	PHE864	5.1625	Hydrophobic	Alkyl
	VAL734	5.20419	Hydrophobic	Pi-Alkyl
	LYS753	4.90467	Hydrophobic	Pi-Alkyl
	VAL734	5.30331	Hydrophobic	Pi-Alkyl
	ALA751	4.61606	Hydrophobic	Pi-Alkyl
	ILE767	4.77372	Hydrophobic	Pi-Alkyl
DB-StigAc	LEU852	5.01603	Hydrophobic	Alkyl
	LEU726	5.42176	Hydrophobic	Alkyl
	LEU852	5.2412	Hydrophobic	Alkyl
	LEU726	4.25717	Hydrophobic	Alkyl
	LEU852	4.81659	Hydrophobic	Alkyl
	LEU726	4.05719	Hydrophobic	Alkyl
	VAL734	3.68654	Hydrophobic	Alkyl
	ALA771	3.38871	Hydrophobic	Alkyl
	VAL734	3.93782	Hydrophobic	Alkyl
	VAL734	4.57731	Hydrophobic	Alkyl

Table 5. *Cont.*

Ligand	Residues	Distance (Å)	Category Bond	Type
DB-StigAc	VAL734	3.94352	Hydrophobic	Alkyl
	ALA751	4.54209	Hydrophobic	Alkyl
	LYS753	4.88391	Hydrophobic	Alkyl
	PHE864	5.44688	Hydrophobic	Pi-Alkyl
	PHE864	4.63064	Hydrophobic	Pi-Alkyl
NorUrsa-Diene	LEU712	5.22621	Hydrophobic	Alkyl
	ARG713	4.78945	Hydrophobic	Alkyl
	ARG784	4.7172	Hydrophobic	Alkyl
	LEU786	5.01266	Hydrophobic	Alkyl
	ARG713	4.07337	Hydrophobic	Alkyl
	ARG784	4.12891	Hydrophobic	Alkyl
	ARG713	4.94763	Hydrophobic	Alkyl
	ARG713	4.97205	Hydrophobic	Alkyl
	ARG784	5.18003	Hydrophobic	Alkyl
Deca-Naph-IMe	ALA771	5.25394	Hydrophobic	Alkyl
	ALA771	4.41343	Hydrophobic	Alkyl
	LEU785	4.99785	Hydrophobic	Alkyl
	LEU796	5.0161	Hydrophobic	Alkyl
	LEU796	5.49973	Hydrophobic	Alkyl
	PHE864	4.80342	Hydrophobic	Pi-Alkyl
	PHE864	5.08466	Hydrophobic	Pi-Alkyl
	LYS753	3.95016	Hydrogen Bond	Conventional Hydrogen Bond
	SER783	2.1716	Hydrogen Bond	Conventional Hydrogen Bond
	THR862	2.60232	Hydrogen Bond	Conventional Hydrogen Bond
	ASP863	3.53282	Hydrogen Bond	Carbon Hydrogen Bond
	ILE767	3.63013	Hydrophobic	Pi-Sigma
	PHE864	4.9441	Hydrophobic	Pi-Pi T-shaped
SNTE	VAL734	4.41465	Hydrophobic	Alkyl
	VAL734	4.20559	Hydrophobic	Alkyl
	VAL734	5.18686	Hydrophobic	Alkyl
	ALA751	4.91575	Hydrophobic	Alkyl
	LEU852	4.80687	Hydrophobic	Alkyl
	LEU726	4.51161	Hydrophobic	Alkyl
	LEU800	5.36538	Hydrophobic	Alkyl
	MET801	5.24233	Hydrophobic	Alkyl
	LEU852	3.09501	Hydrophobic	Alkyl

4. Discussion

The present study investigated the phytochemical composition, Molecular docking, ADME (Absorption, Distribution, Metabolism and Excretion), and toxicity of bioactive compounds in *Dimocarpus longan* leaves against the human epidermal growth factor receptor 2 (HER2) target. The overexpression of HER2 is a characteristic feature of a range of malignancies, especially breast cancer, and its inhibition was one of the key treatment directions [14]. Lapatinib is a dual tyrosine kinase inhibitor (TKI) of HER2 and EGFR, and it is used as a standard reference drug in the study since its efficacy is clinically proven [15]. The phytocompounds identified tentatively through GC–MS, particularly 22,23-dibromostigmasterol acetate, 24-norursa-3,12-diene, succinic acid 2-(3-nitrophenyl)ethyl tridecyl ester, and naphthalene derivatives, were comparatively analyzed to evaluate their potential as alternative HER2 inhibitors.

Lapatinib showed a binding affinity of −10.5 kcal/mol, which established numerous conventional hydrogen bonds, electrostatic interactions, and hydrophobic contacts to HER2 residues including MET801, ASP863, Asp845, LYS753 and PHE864. These reactions are in line with earlier structural investigations that assign the activity of Lapatinib to its quinazoline scaffold and halogen and ether groups that are also capable of hydrogen bond formation and hydrophobic stabilization [16].

While docking provides initial insights to protein-ligand compatibility, it is necessary to consider pharmacokinteic behavior of compounds. The phytochemicals had closest binding affinities with Lapatinib, with dihydroartemisin-t-butyl (−9.3 kcal/mol) and pseudodiosgenin (−9.3 kcal/mol), although 22,23-dibromostigmasterol acetate (−8.9 kcal/mol) and 24-norursa-3,12-diene (−8.6 kcal/mol) also had strong interactions. These compounds were a little weaker than Lapatinib, yet they showed binding energies that suggest that they might be HER2 inhibitors.

Notably, succinic acid 2-(3-nitrophenyl)ethyl tridecyl ester established several strong hydrogen bonds with such residues as LYS753, SER783, and THR862, replicating the binding technique of Lapatinib. This indicates that nitrophenyl and ester functional groups play a role in positive polar interactions; however, long alkyl chain contributes to hydrophobic stabilization.

Conversely, triterpenoid-based counterparts like 24-norursa-3,12-diene were largely dependent on hydrophobic alkyl interactions with residues such as ARG713, LEU786, and ARG784, just as they were lipophilic. Such nonpolar interactions can also be stabilizing but weakly directional, as in Lapatinib. Therefore, these compounds do not necessarily reach the same level of potency, but they might also be effective at HER2 inhibition by being membrane-embedded or allosterically modulated [17,18].

Although docking offers a preliminary measure of the compatibility of ligands and proteins, ADME properties play an important role in determining drug-likeness. The Rule of Five by Lipinski suggests that Lapatinib fails to satisfy one of the requirements since it has a high molecular weight (>500 Da), and this explains to some extent why it does not reach the gastrointestinal (GI) tract and across the blood-brain barrier (BBB). This pharmacokinetic adverse effect is not new to the literature because Lapatinib tends to need to be used with other drugs and the penetration of this drug into the CNS is often limited [19].

Surprisingly, a number of phytochemicals exhibited better ADME properties. In this case, dihydroartemisinin-t-butyl and pseudodiosgenin exhibited a high GI absorption and acceptable lipophilicity, and no or minimal Lipinski violation, which indicates an increase in oral bioavailability relative to Lapatinib. Pregna-5,8-diene-3-benzene-11-alpha-diol-20-one diacetate also had all the parameters, and the intestinal absorption was high (99.2), and no violations were observed. This makes these properties beneficial to clinical translation, since they suggest effective systemic exposure and less reliance on formulation optimization.

Conversely, 22, 23-dibromostigmasterol acetate which had high docking affinity breached two Lipinski rules (molecular weight and lipophilicity) to predict poor oral absorption and low permeability. On the same note, 24-norursa-3,12-diene and decahydro-naphthalene derivatives, which are highly lipophilic compounds, were shown to have low GI absorption and low BBB permeability. This highlights the classic challenge of balancing potency with drug-likeness in natural products: large, lipophilic phytochemicals may bind tightly but face bioavailability constraints [20].

Predictions of toxicity gave additional information on the therapeutic usefulness of phytoligands. Lapatinib reported large hepatotoxicity (0.80), neurotoxicity (0.86), and respiratory toxicity (0.94), which are in line with her reported adverse effects, which are hepatobiliary dysfunction and pulmonary complications in the clinic [21]. Besides, its immunotoxicity score (0.96) is high, which is in line with immune side effects that are associated with the use of kinase inhibitors.

Of the phytochemicals, 22, 23-dibromostigmasterol acetate exhibited immunotoxicity (0.99) and possible carcinogenicity indicating that it is not very safe when used in the systemic application. In contrast, 24-norursa-3, 12-diene and naphthalene derivatives were found to exhibit low organ toxicity, no active hepatotoxicity and no active mutagenicity. The influence of this low toxicity profile in combination with moderate binding affinity is that they have potential as lead compounds to be optimized. The derivatives of succinic acids showed an ambiguous image, low hepatotoxicity, but the mutagenicity was anticipated, probably due to the nitrophenyl group. These structural warnings should be taken seriously and a logical adjustment implemented to remove toxicophores.

The comparative study of functional groups demonstrates the mechanistic nature of the activity of the ligands. The quinazoline core of Lapatinib and anilino substituents permit π -decades of the molecule with aromatic residues as well as hydrogen bonding with the amino acids of the hinge region of HER2. It has more polarity by having fluorophenyl and ether functional groups, which increases binding specificity [22]. In the case of phytochemicals, triterpenoids like pseudodiosgenin and 24-norursa-3,12-diene do not have strong polar groups, but have rigid ring systems to stabilise hydrophobic interactions [23]. These sterol-like molecules mainly fix in the nonpolar cavity of HER2 indicating a different mechanism of inhibition as compared to Lapatinib. Artemisinin derivatives such as dihydroartemisinin-t-butyl have peroxide bridges and hydroxyl groups that promote hydrogen bonding, which could be the reason why they have good docking scores and pharmacokinetics [24]. Aromatic nitro group and long aliphatic chains are bonded to succinic acid esters and offer hydrogen bond as well as hydrophobic anchor. The nitro group is however, a two-sided sword, where one can interact strongly at the cost of mutagenic danger [25].

Thus, SAR analysis suggests that the combination of polar function groups (to mimic Lapatinib's hinge-binding) with optimized hydrophobic scaffolds (to utilize phytochemical scaffolds) will lead to efficient and safer HER2 inhibitors [26]. Mechanistically, Lapatinib inhibits HER2 signaling through occupying the ATP-binding cleft within the kinase domain, inhibiting phosphorylation and subsequent activation of PI3K/AKT and MAPK

pathways [27]. Phytochemicals elucidated here have the potential to act through similar competitive inhibition of HER2 ATP binding, as evidenced by docking into the same catalytic pocket.

Furthermore, lipophilic triterpenoids could also interfere with dimerization or lipid raft recruitment of the receptor, indirectly inhibiting HER2 signaling. Compounds like dihydroartemisinin derivatives could possess dual mechanisms, maintaining direct kinase inhibition alongside the generation of reactive oxygen species (ROS) triggering apoptosis in HER2 overexpression cells [28]. Therefore, the multi-target potency of phytochemicals could provide higher anticancer activity, circumventing Lapatinib monotherapy resistance mechanisms.

While reporting encouraging *in silico* findings, there are a number of gaps in here. First, the docking study was limited to HER2, but in vivo HER2-positive tumors usually have compensatory signaling through HER3 and EGFR. Multi-target docking must therefore be performed to account for network-level blockade. Second, ADME predictions, while valuable, must be validated by in vitro permeability tests (e.g., Caco-2 monolayers) and metabolic stability experiments. Third, toxicology predictions must be demonstrated experimentally, particularly for nitroaromatic compounds with mutagenicity notices.

In addition, structural diversity of phytochemicals necessitates rational derivatization to enhance drug-likeness. Modification of triterpenoid skeletons by semi-synthetic means could involve incorporation of hydrogen bond donors/acceptors, while artemisinin skeletons can be hybridized with quinazoline moieties to mimic the hinge-binding of Lapatinib with retained natural product bioactivity.

Finally, synergistic potential should not be ruled out. Combining phytoligands with Lapatinib would lower the dose that is actually required, thereby minimizing toxicity while still providing HER2 blockade. Combination methodologies of such a type are particularly relevant in high-impact oncology research, where multi-faceted treatment is becoming more desirable.

5. Conclusions

This study highlights that phytochemicals derived from *Dimocarpus longan* leaves, particularly dihydroartemisinin-t-butyl, pseudodiosgenin, 24-norursa-3,12-diene, and succinic acid derivatives, demonstrate noteworthy HER2 binding, favorable ADME properties, and in some cases lower toxicity than the reference drug Lapatinib. While none surpassed Lapatinib in docking affinity, their superior pharmacokinetics and reduced predicted toxicity suggest potential as lead scaffolds for next-generation HER2 inhibitors. Rational optimization, mechanistic validation, and synergistic evaluation with existing TKIs are essential next steps. By bridging natural product chemistry with targeted oncology, these findings open avenues for developing safer, bioavailable, and multi-targeted therapies for HER2-positive cancers.

Author Contributions

M.F.R. (Md. Fozla Rabby) and M.F.R. (Md. Foyzur Rahman): Data curation, methodology, formal analysis, investigation, conceptualization; software, investigation; visualization, data analysis, formal analysis, writing-original draft preparation. A.-S.M. and A.B.: Data analysis, formal analysis, supervision, writing-review and editing, conceptualization, methodology, formal analysis, investigation, supervision, writing-review and final editing. All authors have read and agreed to the published version of the manuscript.

Funding

This research received no external funding.

Institutional Review Board Statement

Not applicable.

Informed Consent Statement

Not applicable.

Data Availability Statement

The data presented in this study are available from the corresponding author upon reasonable request.

Conflicts of Interest

The authors declare no conflict of interest.

Use of AI and AI-Assisted Technologies

The authors confirm that no AI tools or AI-assisted technologies were used in the preparation of this manuscript.

References

1. Kim, J.; Harper, A.; McCormack, V.; et al. Global patterns and trends in breast cancer incidence and mortality across 185 countries. *Nat. Med.* **2025**, *31*, 1154–1162.
2. Liao, L. Inequality in breast cancer: Global statistics from 2022 to 2050. *Breast* **2025**, *79*, 103851.
3. Wang, J.; Xu, B. Targeted therapeutic options and future perspectives for HER2-positive breast cancer. *Signal Transduct. Target. Ther.* **2019**, *4*, 34.
4. Giuliano, M.; Trivedi, M.V.; Schiff, R. Bidirectional crosstalk between the estrogen receptor and human epidermal growth factor receptor 2 signaling pathways in breast cancer: Molecular basis and clinical implications. *Breast Care* **2013**, *8*, 256–262.
5. Sikdar, N.; Saha, G.; Dutta, A.; et al. Genetic alterations of periampullary and pancreatic ductal adenocarcinoma: An overview. *Curr. Genomics* **2018**, *19*, 444–463.
6. Slamon, D.J.; Clark, G.M.; Wong, S.G.; et al. Human breast cancer: Correlation of relapse and survival with amplification of the HER-2/neu oncogene. *Science* **1987**, *235*, 177–182.
7. Gezici, S.; Şekeroğlu, N. Current perspectives in the application of medicinal plants against cancer: Novel therapeutic agents. *Anti-Cancer Agents Med. Chem.* **2019**, *19*, 101–111.
8. Ilaro, F.P. In silico anticancer assessment of the bioactive compounds of *Aframomum melegueta* on HER2 protein associated with breast cancer. *Int. J. Women Tech. Educ. Employ.* **2023**, *4*, 1–15.
9. Govindappa, M. A review on role of plant extracts and their phytochemicals for the management of diabetes. *J. Diabetes Metab.* **2015**, *6*, 7.
10. Bolaji, O.Q.; Adelusi, T.I.; Ojo, T.O.; et al. Leveraging computational approaches in identifying novel HER2+ breast cancer potential therapeutics: Integrating virtual screening and molecular dynamics simulation. *Future J. Pharm. Sci.* **2025**, *11*, 1.
11. Bose, R.; Kavuri, S.M.; Searleman, A.C.; et al. Activating HER2 mutations in HER2 gene amplification-negative breast cancer. *Cancer Discov.* **2013**, *3*, 224–237.
12. Bilancia, D.; Rosati, G.; Dinota, A.; et al. Lapatinib in breast cancer. *Ann. Oncol.* 2007, 18, vi26–vi30.
13. Elekofehinti, O.O.; Ejelonu, O.C.; Kamdem, J.P.; et al. Discovery of potential visfatin activators using in silico docking and ADME predictions as therapy for type 2 diabetes. *Beni-Suef Univ. J. Basic Appl. Sci.* **2018**, *7*, 241–249.
14. Ramasamy, S.; Jeyaram, K.; Narayanan, A.; et al. Repurposing fluvoxamine as an inhibitor for NUDT5 in breast cancer cells: An in silico and in vitro study. *In Silico Pharmacol.* **2024**, *13*, 5.
15. Medina, P.J.; Goodin, S. Lapatinib: A dual inhibitor of human epidermal growth factor receptor tyrosine kinases. *Clin. Ther.* **2008**, *30*, 1426–1447.
16. Elkamhawy, A.; Son, S.; Lee, H.Y.; et al. Design, synthesis, biological evaluation, and molecular dynamics studies of novel lapatinib derivatives. *Pharmaceuticals* **2022**, *16*, 43.
17. Abramson, H.N. The lipogenesis pathway as a cancer target. *J. Med. Chem.* **2011**, *54*, 5615–5638.
18. Aertgeerts, K.; Skene, R.; Yano, J.; et al. Structural analysis of the mechanism of inhibition and allosteric activation of the kinase domain of HER2 protein. *J. Biol. Chem.* **2011**, *286*, 18756–18765.
19. Karbownik, A.; Sobańska, K.; Płotek, W.; et al. The influence of the coadministration of the P-glycoprotein modulator elacridar on the pharmacokinetics of lapatinib and its distribution in the brain and cerebrospinal fluid. *Investig. New Drugs* **2020**, *38*, 574–583.
20. Aqil, F.; Munagala, R.; Jeyabalan, J.; et al. Bioavailability of phytochemicals and its enhancement by drug delivery systems. *Cancer Lett.* **2013**, *334*, 133–141.
21. Zhou, Y.; Gong, J.; Deng, X.; et al. A comprehensive exploration of adverse reactions to lapatinib: A disproportionate analysis based on the FAERS database. *Expert Opin. Drug Saf.* **2025**, *24*, 1521–1530.
22. Elwaie, T.A.; Abbas, S.E.; Aly, E.I.; et al. HER2 kinase-targeted breast cancer therapy: Design, synthesis, and in vitro and in vivo evaluation of novel lapatinib congeners as selective and potent HER2 inhibitors with favorable metabolic stability. *J. Med. Chem.* **2020**, *63*, 15906–15945.
23. Ghosh, S. Triterpenoids: Structural diversity, biosynthetic pathway, and bioactivity. *Stud. Nat. Prod. Chem.* **2020**, *67*, 411–461.
24. White, N.J. Clinical pharmacokinetics and pharmacodynamics of artemisinin and derivatives. *Trans. R. Soc. Trop. Med. Hyg.* **1994**, *88*, 41–43.

25. Tinkov, O.V.; Ognichenko, L.N.; Kuz'min, V.E.; et al. Computational assessment of environmental hazards of nitroaromatic compounds: Influence of the type and position of aromatic ring substituents on toxicity. *Struct. Chem.* **2016**, *27*, 191–198.
26. Shipunova, V.O.; Kolesnikova, O.A.; Kotelnikova, P.A.; et al. Comparative evaluation of engineered polypeptide scaffolds in HER2-targeting magnetic nanocarrier delivery. *ACS Omega* **2021**, *6*, 16000–16008.
27. Shi, H.; Zhang, W.; Zhi, Q.; et al. Lapatinib resistance in HER2+ cancers: Latest findings and new concepts on molecular mechanisms. *Tumour Biol.* **2016**, *37*, 15411–15431.
28. Dai, X.; Zhang, X.; Chen, W.; et al. Dihydroartemisinin: A potential natural anticancer drug. *Int. J. Biol. Sci.* **2021**, *17*, 603.